Contents lists available at Science-Gate

International Journal of Advanced and Applied Sciences

Journal homepage: http://www.science-gate.com/IJAAS.html

Statistical edge detection with an application to intraventricular hemorrhage

Sameer A. H. Al-Subh *, Kamal A. Al-Banawi

Department of Mathematics and Statistics, Mutah University, Al-Karak, Jordan

ARTICLE INFO

Article history:
Received 21 May 2024
Received in revised form
14 September 2024
Accepted 28 October 2024

Keywords:
Edge detection
Derivative operators
Threshold
Canny edge detector
Intraventricular hemorrhage

ABSTRACT

The goal of edge detection is to determine whether a point in an image is an edge point. This is done by applying first and second derivative operators to detect the greatest change in image intensity. In this paper, we propose a new method where the threshold, represented by the average $\bar{a}$, is calculated within a neighborhood of $I(x_1,x_2)$. This approach not only reduces processing time but also ensures that no pixels are missed. Pixels below the threshold are replaced after enhancement. We extend this work by applying the Canny edge detector (CED) to detect boundaries in MRI images of abnormal brains affected by intraventricular hemorrhage (IVH). Two thresholds are used: the hysteresis threshold in the CED and our proposed statistical threshold, which works alongside traditional edge operators like Sobel, Prewitt, and Laplacian.

1. Introduction

In recent years, advances in medical imaging technology have greatly improved the use of medical images in patient diagnosis. MRI images have become a key tool for clinical diagnosis and treatment. However, the quality of these images can influence medical assessments and is often affected by noise, image distortions, and human factors. As a result, the edges in MRI images may appear unclear, making it challenging for the human eye to discern subtle details accurately. Therefore, thorough research into effective edge detection methods for MRI images is essential, with statistical approaches being particularly recommended. In our study, we focus on detecting edges in images of Intraventricular Hemorrhage (IVH) using the Canny edge detection operator (Canny, 1986).

Shokhan (2014) recommended an improved Canny edge detection algorithm, which can better detect the edges of low-resolution angiograph images. Mao (2017) solved the problem of edge detection in medical images based on an improved bacterial chemotaxis-based ant colony algorithm. Qian (2019) used an adaptive median filter to denoise, the Sobel operator to calculate gradient magnitude direction, to refine image non-maximum suppression, OSTU to calculate high and low thresholds to improve the Canny operator, and to conduct experiments on medical images.

You et al. (2023) explored the application of the wavelet transform modulus maxima method combined with the OTSU thresholding technique for edge detection, demonstrating improved performance in images with complex backgrounds. The authors highlight the method's effectiveness in enhancing detection quality and efficiency, making it a valuable reference for contemporary edge detection research. Sun et al. (2022) provided an extensive overview of edge detection techniques, covering both traditional methods and recent advancements in deep learning approaches, offering valuable insights into the evolution and current state of edge detection algorithms. Zhou and Yuan (2024) introduced a biorthogonal cubic special spline wavelet designed to enhance edge detection in images, particularly in noisy environments. The proposed method effectively addresses noise while preserving edge details, offering a robust solution for edge detection tasks. An improved edge detection method for medical images based on fractional differential algorithm and the experimental results show that the method not only effectively extracts image edge features but also has a good inhibitory effect on noise. Jogi and Srinivasa Rao (2022) presented an enhanced edge detection technique that combines adaptive thresholding with morphological operations to improve the accuracy of edge detection in medical images. The method focuses on refining edge detection by addressing issues related to noise and varying image intensities.

* Corresponding Author.
Email Address: salsubh@mutah.edu.jo (S. A. H. Al-Subh)
https://doi.org/10.21833/ijaas.2024.11.010
Corresponding author's ORCID profile:
https://orcid.org/0009-0006-2973-6929

Liu et al. (2011) proposed a morphological edge detection method using multi-structuring elements and multi-scale morphology based on image fusion within the wavelet domain, enhancing the extraction of edge information for more accurate detection results. Tan et al. (2020) proposed a novel multimodal medical image fusion algorithm that utilizes multi-scale morphological gradient operators to extract gradient information, indicating contrast intensity in the neighborhood of a pixel. The method effectively enhances edge detection and noise suppression in medical images, aligning with the principles of multi-scale morphological entropy-based edge detection. Gao et al. (2010) proposed an improved Sobel edge detection method that enhances the traditional Sobel operator by optimizing the gradient thresholding and incorporating new techniques to achieve more accurate and robust edge detection results. Wang and Ma (2024) presented a super-resolution reconstruction algorithm for medical images that combines wavelet transform with multi-scale adaptive feature selection. The method effectively enhances edge detection and improves the quality of 3D medical image reconstruction, addressing challenges in accurately extracting edges from complex medical images. Alnaggar et al. (2024) comprehensively reviewed various artificial intelligence techniques, including intelligent algorithms for edge detection, applied to medical image analysis. It provides insights into the efficiency, computational complexities, and scalability of these approaches, highlighting advancements in optimizing edge detection in medical imaging. Cao (2019) projected that the Canny edge detection algorithm is very suitable for medical image processing and has considerable significance in this field. Lu et al. (2023) integrated the Sobel operator with multi-attention segmentation networks to enhance edge detection and segmentation accuracy in medical images, demonstrating the practical significance of the Sobel operator in medical image analysis and retrieval. Trujillo-Pino et al. (2013) discussed techniques for accurate subpixel edge detection, focusing on enhancing precision, which could be relevant to algorithms like morphological gradients and Zernike moments applied to edge detection tasks.

Edge detection operators are commonly used in image processing to create new images with sharp, well-defined boundaries from existing ones. Edges are identified by locating pixels where the intensity changes significantly relative to their surrounding neighborhood. These changes are calculated and used to detect edges through gradient and difference-based operators, which rely on the first and second derivatives of image intensity.

If “I” denotes the intensity function defined on the 2-dimensional array of the image, then “I” is a two variable real function $I(x_1, x_2)$. Let I_{x_1} and I_{x_2} be the partial derivatives of “I” with respect to x_1 and x_2 respectively. Then ∇I, the gradient vector of the intensity function “I”, is given by $\nabla I = I_{x_1}\hat{\imath} + I_{x_2}\hat{\jmath}$ where $\hat{\imath}, \hat{\jmath}$ are the usual coordinate unit vectors (Corwin and Szczarba, 1979; Adams, 1995). Let $\|\nabla I\|$ be the magnitude of the gradient, then $\|\nabla I\| = \sqrt{I_{x_1}^2 + I_{x_2}^2}$.

The change in $I(x_1, x_2)$ is usually expressed by $\|\nabla I\|$, hence the maximum value of the change of intensity is the maximum value of the gradient. This means that an edge is present if the gradient value of the intensity function is maximum or if the gradient value surpasses a certain threshold. Since the domain of digital images is discrete, the partial derivatives in the magnitude of the gradient can be approximated by simple first differences. It is the formula for the first differences that distinguishes one operator from another.

The first step in constructing an edge operator is selecting an appropriate neighborhood size around a point in the image, typically using a 2×2 or 3×3 block. This neighborhood consists of a set of points defined relative to the central image point. In image processing, the neighborhood may include or exclude the central point and can contain points that are not necessarily adjacent. To approximate the derivative, intensity values from the neighborhood are used to calculate simple first differences. A matrix is then created to represent these values, matching the neighborhood's size. The elements of this matrix are derived from coefficients corresponding to terms in the neighborhood, with any term not appearing represented as zero. This matrix is referred to as the convolution kernel (or mask) for estimating the partial derivative. Convolution involves placing an n×n operator over an n×n neighborhood in the image, multiplying corresponding values, and summing the results (Miller and Zeuch, 1989). The approximation results are derived using convolution kernels, and these results are then combined point by point using a suitable method to obtain the final gradient estimate. Typically, when approximating the gradient, two values, V_1 and V_2, are used. There are two common methods for calculating the magnitude of the gradient at an image point: the root mean square (RMS) method and the absolute value (AV) method. In the RMS method, the values V_1 and V_2 are combined as $V = \sqrt{V_1^2 + V_2^2}$. In the AV method, they are combined as $V = |V_1| + |V_2|$.

The most well-known first derivative directional operators are the Prewitt and Sobel operators (Prewitt, 1970). Prewitt uses the neighborhood:

$f(x_1-1, x_2-1)$	$f(x_1-1, x_2)$	$f(x_1-1, x_2+1)$
$f(x_1, x_2-1)$	$f(x_1, x_2)$	$f(x_1, x_2+1)$
$f(x_1+1, x_2-1)$	$f(x_1+1, x_2)$	$f(x_1+1, x_2+1)$

The two values used here are:

$$V_1 = f(x_1+1, x_2-1) + f(x_1+1, x_1) + f(x_1+1, x_2+1) \\ - f(x_1-1, x_2-1) - f(x_1-1, x_2) \\ - f(x_1-1, x_2+1),$$

$$V_2 = f(x_1-1,x_2+1) + f(x_1,x_2+1) + f(x_1+1,x_2+1) - f(x_1-1,x_2-1) - f(x_1,x_2-1) - f(x_1+1,x_2-1).$$

The convolution kernels are $\begin{pmatrix} -1 & -1 & -1 \\ 0 & 0 & 0 \\ 1 & 1 & 1 \end{pmatrix}$ and $\begin{pmatrix} -1 & 0 & 1 \\ -1 & 0 & 1 \\ -1 & 0 & 1 \end{pmatrix}$.

Sobel uses Prewitt's neighborhood with the values:

$$V_1 = f(x_1+1,x_2-1) + 2\,f(x_1+1,x_2) + f(x_1+1,x_2+1) - f(x_1-1,x_2-1) - 2f(x_1-1,x_2) - f(x_1-1,x_2+1),$$
$$V_2 = f(x_1-1,x_2+1) + 2\,f(x_1,x_2+1) + f(x_1+1,x_2+1) - f(x_1-1,x_2-1) - 2f(x_1,x_2-1) - f(x_1+1,x_2-1).$$

So that his convolution kernels are $\begin{pmatrix} -1 & -2 & -1 \\ 0 & 0 & 0 \\ 1 & 2 & 1 \end{pmatrix}$ and $\begin{pmatrix} -1 & 0 & 1 \\ -2 & 0 & 2 \\ -1 & 0 & 1 \end{pmatrix}$.

Edge points are detected here by using the second derivative of the image intensity function. Let $I_{x_1x_1}$ *and* $I_{x_2x_2}$ be the second-order unmixed partial derivatives of the intensity function I, then the Laplacian serves as the two-dimensional equivalent of the second derivative (Davis and Snider, 1995). The formula for the Laplacian of the intensity function is $\nabla I^2 = I_{x_1x_1} + I_{x_2x_2}$. A second derivative operator that approximates the Laplacian is derived using a sufficient assumption for an approximation to the first derivative. If I_{x_1} is approximated by $I(x_1,x_2+1) - I(x_1,x_2)$, then:

$$I_{x_1x_1} = I(x_1,x_2+1) - 2I(x_1,x_2) + I(x_1,x_2-1) \quad (1)$$

Is the desired approximation for the second partial derivative centered around (x_1,x_2). Similarly,

$$I_{x_2x_2} = I(x_1+1,x_2) - 2I(x_1,x_2) + I(x_1-1,x_2) \quad (2)$$

By combining the last two approximations into a single one, the Laplacian can be put in the approximated form:

$$\nabla I^2 \approx I(x_1,x_2+1) + I(x_1,x_2-1) + I(x_1+1,x_2) + I(x_1-1,x_2) - 4I(x_1,x_2) \quad (3)$$

Thus, a 3×3 neighborhood centered about $f(x_1,x_2)$ - as in Prewitt or Sobel (Prewitt, 1970)- is processed by the convolution kernel $\begin{pmatrix} 0 & 1 & 0 \\ 1 & -4 & 1 \\ 0 & 1 & 0 \end{pmatrix}$.

While edge detection in statistics exploits the idea of hypothesis testing, different methods are used in voting. For example, during the computation of the decision rule, Huang and Tseng (1988) used the mean and variance of the neighborhood for split and merge analysis. In our work, the threshold is the average intensity in the neighborhood of the pixel.

2. Thresholding

When using first derivative operators, an edge is identified if the gradient magnitude exceeds a certain threshold. The goal is to choose a threshold such that pixels with values below it are set to zero, while those with values above it are set to one. It may be necessary to perform the edge detection test multiple times with different threshold assumptions to achieve the desired image shape. To avoid making arbitrary threshold choices, an alternative approach called the iterative threshold selection (ITS) can be used. This method starts by selecting an initial threshold and then iteratively refines it to find an optimal value. Usually, the initial value is chosen as the statistical mean of the integers in the array after estimating the gradient (Wei et al., 2022; She, 2009).

In order to implement and validate our proposed edge detection methods, we developed a series of programs using Matlab. These programs utilize established convolution operators and novel thresholding techniques to process and analyze image data effectively. Below, we outline key functions demonstrating how the Prewitt, Sobel, and Laplacian operators were applied in our approach.

```
Prewitt Operator
function [p]=prewitt (a)
P1= [1 1 1; 0 0 0; -1 -1 -1];
P2= [1 0 -1; 1 0 -1; 1 0 -1];
% p1 and p2 are the convolution kernels (masks).
h= conv2 (a, p1);
v=conv2(a,p2);
grad=sqrt (h.^2+v.^2);
% The gradient is estimated using the RMS method.
P=floor (grad);
Sobel Operator
function [s]=sobel (a)
s1=[1 2 1; 0 0 0; -1 -2 -1];
s2=[1 0 -1; 2 0 -2; 1 0 -1];
% s1 and s2 are the convolution kernels (masks).
h=conv2 (a,s1);
v=conn2 (a,s2);
Grad=sqrt(h.^2+v.^2);
% The gradient is estimated using the RMS method.
s=floor (grad);

Thresholding
function [th]=threshold (a1)
[m1,n1]=size (a1);
s=0;
for i=1:m1
   for j=1:n1
        s=s+a1 (i,j);
     end
 end
th=s/(m1*n1);
v=th-2;
s1=0; s2=0; k1=0; k2=0;
while th~=v
       for i=1:m1
          for j=1:n1
               if a1(i,j)<=th
                  s1=s1+a1(i,j);
                   k1=k1+1;
               else
                s2=s2+a1(i,j);
```

```
                k2=k2+1;
            end
        end
end
v1=s1/k1;
v2=s2/k2;
v=(v1+v2)/2;
if th~=v;
   th=v;
   v=th-2;
s1=0;s2=0;k1=0;k2=0;
    end
end
th=v;
Edge Detection
function [fed] =firstedgedet (a1, th)
% Edge detection using the threshold th.
[m1,n1] =size (a1);
fed=zeros (m1, n1);
for i=1:m1
   for j=1:n1
      if a1 (i, j) >=th
         fed (i, j) =1;
        end
    end
end
imshow (fed)
The Laplacian Operator
function [l]= laplacian (a)
lap= [0 1 0; 1 -4 1; 0 1 0];
% lap is the convolution kernel (mask)
v=conv2 (a, lap);
% The image is edge detected.
l=floor (v);
Imshow (l)
```

3. Statistical edge detection

In Lim (2006), the author described an edge detector founded on the robust rank order (RRO) test, specifically designed for noisy images. His method is based on testing whether an $n \times n$ convolution matrix is portioned into two submatrices having real differences in local gray-level values between pixels in that matrix. Through the application of the Wilcoxon test, T-test, the Canny Edge Detector (CED) (Canny, 1986), and the RRO detector, experiments were conducted on real images corrupted by noise.

Ünver et al. (2019) calculated the mean brightness (MB) level of the image to streamline computational time. The MB value served as a threshold, with pixels below this value being removed from the image. The calculation of the MB level by Ünver et al. (2019) is determined by

$$\text{Threshold Level} = \frac{1}{M\times N}\sum_{i=1}^{M}\sum_{j=1}^{N} Img(i,j) \qquad (4)$$

where, $M \times N$ is the size of the image.

We consider a small section of the noisy image represented by $n \times n$ neighborhood, where n is an odd number, with a point of interest $I(x_1, x_2)$ centered within it. Let $\delta > 0$. The $(n \times n) - 1$ gray level values are then divided into two categories: $\mathcal{A} = \{a_1, \dots, a_{r_1}\}$ and $\mathcal{B} = \{b_1, \dots, b_{r_2}\}$, where $r_1 + r_2 = (n \times n) - 1$, while

$$|I(x_1, x_2) - a_k| < \delta, \quad |I(x, y) - b_m| \geq \delta, k = 1, \dots, r_1, m = 1, \dots, r_2.$$

Let $\bar{a} = \frac{\sum_{k=1}^{r_1} a_k}{r_1}$. Then, in our work, the threshold is the average $\bar{a}$ in a neighborhood of $I(x_1, x_2)$, which saves more time, and no pixels are omitted. In fact, pixels below the threshold value are replaced by new ones after enhancement.

Presently, our focus lies in testing the null hypothesis:

$$H_0: |I(x_1, x_2) - a_k| < \delta$$

against the alternative hypothesis,

$$H_1: |I(x_1, x_2) - a_k| \geq \delta \qquad (5)$$

for the set $\mathcal{A}$. Similarly, we can do another test for the set $\mathcal{B}$, here,

$$H_0: |I(x_1, x_2) - b_k| \geq \delta$$

against,

$$H_1: |I(x_1, x_2) - a_k| < \delta \qquad (6)$$

Take $C_k = \begin{cases} a_k, & a_k \in \mathcal{A} \\ b_k, & b_k \in \mathcal{B} \end{cases}$. To evaluate H_0, we calculate the difference between the gray values. Then,

$a_k \in \mathcal{A}$ if $|I(x_1, x_2) - a_k| < \delta$, otherwise $b_k \in \mathcal{B}$.

Now, we compute the mean of the gray values in the set $\mathcal{A}$, which is $\tilde{a} = \frac{\sum_{k=1}^{r} a_k}{r}$ where $r = \frac{(n\times n)-1}{2}$.

Also $\tilde{b} = \frac{\sum_{k=1}^{r} b_k}{r}$. Take $V_a = \sum_{k=1}^{r}(a_k - \tilde{a})^2$ and $V_b = \sum_{k=1}^{r}\left(b_k - \tilde{b}\right)^2$. After getting test parameters and the homogeneity index of variances, the test statistic is given by,

$$T_A = \frac{r\,\tilde{a} - r\,\tilde{b}}{2\sqrt{V_a + V_b + \tilde{a}\tilde{b}}} \qquad (7)$$

Similarly, T_B can be calculated. Now, we reject H_0 for large values of,

$$T^* = max.(T_A, T_B) \qquad (8)$$

Then, we detect an edge if $T^* > t_\alpha$, for a specified threshold t_α at a significant level α. The algorithm for detecting an edge if $T^* > t_\alpha$, for a indicated threshold t_α at a significant level α is as follows.

Algorithm: Statistical edge detection algorithm

- Step1: Consider a gray scale image Img.
- Step2: For each pixel Img(i, j)of the image Img.
- Step2.1: Find the 5×5 mask centering Img(i, j).
- Step2.2: Find s=sum of intensities of all the pixels of the mask except Img(i, j).
- Step2.3: Calculate avg=s/24.
- Step2.4: Set p=0 and for each pixel in that 5×5 mask except the center pixel

- Increase p by 1 if the pixel has a difference of intensity with $(i, j)^{th}$ pixel less than or equal to δ.
- Step2.5: If $|Img(i, j) - a_k| < \delta$ then accept; Otherwise reject.

4. Canny edge detector on IVH

The Canny operator detects continuous and detailed edges quickly and efficiently. It is commonly used for detecting edges in MRI images (Yunhong et al., 2022). In our work, we compare the performance of the Canny operator with other edge detection methods, such as Sobel, Prewitt, and Laplacian operators, noting that the Canny operator processes images in less than one-third of the time required by the others. Compared to other techniques, it also offers faster computational times and lower memory usage.

IVH refers to bleeding within the cerebral ventricular system and can be classified as either minimal (primary) or extensive (secondary) (Arboix et al., 2012). Our work focuses on detecting edges in IVH images and comparing these results with normal images using the Canny edge operator (Canny, 1986).

The CED is a multi-step algorithm for detecting edges in an input image. It involves calculating the first derivative of the Gaussian function to optimize both the signal-to-noise ratio and edge localization. The CED employs Hysteresis Thresholding to retain pixels with a gradient magnitude above a defined threshold while discarding those below a lower threshold. In our application, we use a threshold value of 7.

Finally, Figs. 1 to 10 show a normal brain and an abnormal brain IVH before and after Canny edge detection. While Fig. 1 and Fig. 2 show a normal brain and an abnormal brain before Canny edge detection, respectively, the edge detection results by the Canny operator for both are shown in Fig. 3 and Fig. 4. Also, it is worth that to see how the original images look like after Sobel, Prewitt and Laplacian operators. Fig. 5 and Fig. 6 show normal brain and an abnormal brain with IVH after Sobel edge detection. Fig. 7 and Fig. 8 show normal brain and an abnormal brain with IVH after Prewitt edge detection. Fig. 9 and Fig. 10 show normal brain and an abnormal brain with IVH after Laplacian edge detection.

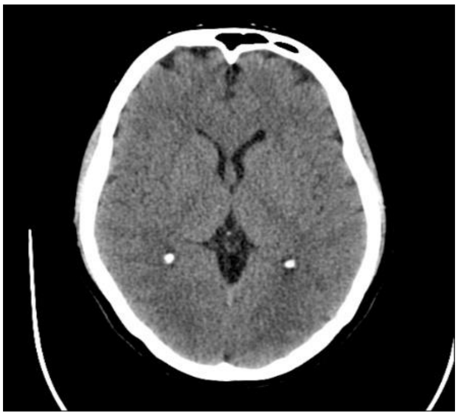

Fig. 1: A normal brain before Canny edge detection

Fig. 2: An abnormal brain with IVH before Canny edge detection

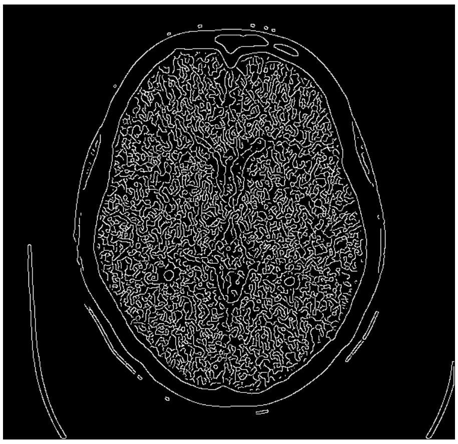

Fig. 3: A normal brain after Canny edge detection

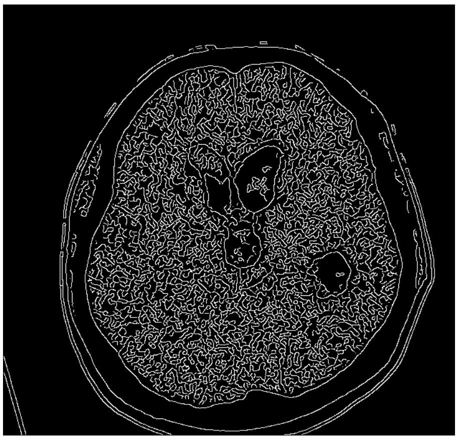

Fig. 4: An abnormal brain with IVH after Canny edge detection

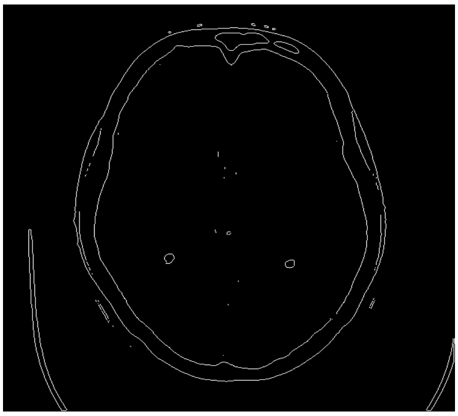

Fig. 5: A normal brain after Sobel edge detection

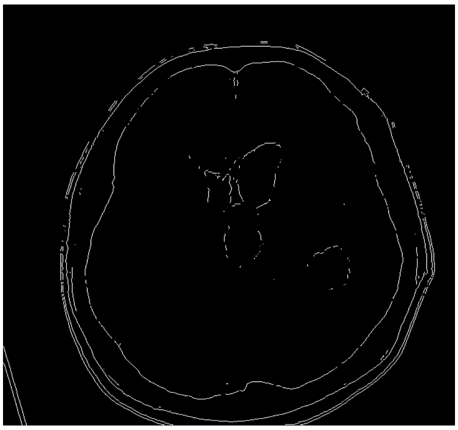

Fig. 6: An abnormal brain with IVH after Sobel edge detection

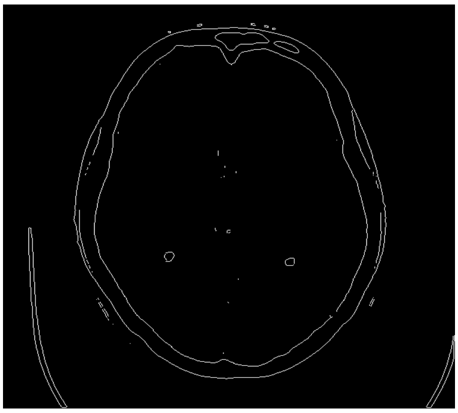

Fig. 7: A normal brain after Prewitt edge detection

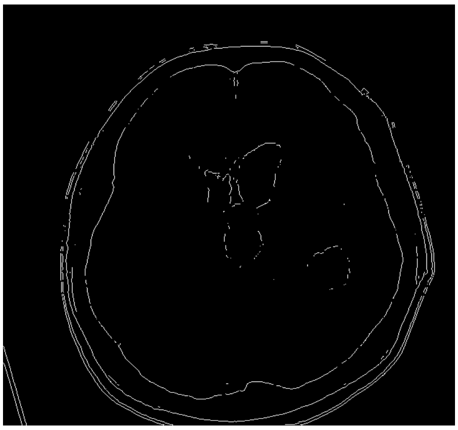

Fig. 8: An abnormal brain with IVH after Prewitt edge detection

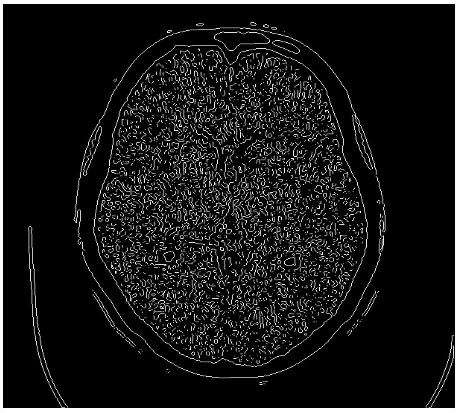

Fig. 9: A normal brain after Laplacian edge detection

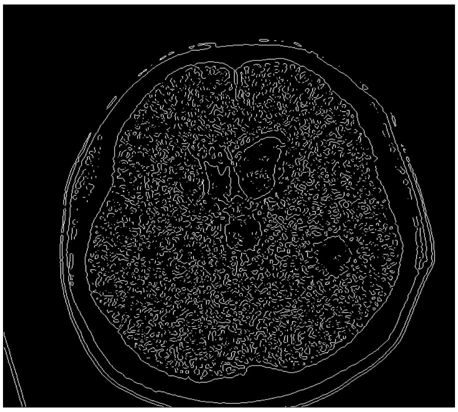

Fig. 10: An abnormal brain with IVH after Laplacian edge detection

5. Conclusion

In this study, we achieved two primary objectives. The first was to introduce a new statistical threshold for edge detection by using the average value $\bar{a}$ of the gray values within a neighborhood after testing the null hypothesis against the alternative hypothesis. The second objective was to apply the CED to enhance images of IVH using Hysteresis Thresholding, demonstrating that our new statistical threshold produced similar results when compared to traditional edge detection methods such as Sobel, Prewitt, and Laplacian operators. Compared to other techniques, the Canny edge detector offers faster processing times and requires less memory.

Compliance with ethical standards

Conflict of interest

The author(s) declared no potential conflicts of interest with respect to the research, authorship, and/or publication of this article.

References

Adams RA (1995). Calculus of several variables. 3rd Edition, Addison Wesley Publishing Company, Boston, USA.

Alnaggar OA, Jagadale BN, Saif MA, Ghaleb OA, Ahmed AA, Aqlan HA, and Al-Ariki HD (2024). Efficient artificial intelligence approaches for medical image processing in healthcare: Comprehensive review, taxonomy, and analysis. Artificial Intelligence Review, 57: 221. https://doi.org/10.1007/s10462-024-10814-2

Arboix A, García-Eroles L, Vicens A, Oliveres M, and Massons J (2012). Spontaneous primary intraventricular hemorrhage: Clinical features and early outcome. International Scholarly Research Notices, 2012: 498303. https://doi.org/10.5402/2012/498303 **PMid:22966468 PMCid:PMC3433135**

Canny J (1986). A computational approach to edge detection. IEEE Transactions on Pattern Analysis and Machine Intelligence, 8(6): 679-698. https://doi.org/10.1109/TPAMI.1986.4767851

Cao YN (2019). Application of canny edge detection algorithm based on Gaussian filter in medical images. Chinese Journal of Endemic Disease Control, 34(5): 54-55.

Corwin LJ and Szczarba RH (1979). Calculus in vector spaces. M. Dekker, New York, USA.

Davis HF and Snider AD (1995). Introduction to vector analysis. William C. Brown Publisher, Dubuque, USA.

Gao W, Zhang X, Yang L, and Liu H (2010). An improved Sobel edge detection. In the 3rd International conference on computer science and information technology 5: 67-71. IEEE, Chengdu, China. https://doi.org/10.1109/ICCSIT.2010.5563693

Huang JS and Tseng DH (1988). Statistical theory of edge detection. Computer Vision, Graphics, and Image Processing, 43(3): 337-346. https://doi.org/10.1016/0734-189X(88)90087-4

Jogi MK and Srinivasa Rao Y (2022). Gray scale image enhancement with CPSO algorithm for medical applications. In: Sharma H, Shrivastava V, Kumari Bharti K, and Wang L (Eds.), Communication and intelligent systems. Lecture notes in networks and systems, Vol 461. Springer, Singapore, Singapore. https://doi.org/10.1007/978-981-19-2130-8_68

Lim DH (2006). Robust edge detection in noisy images. Computational Statistics and Data Analysis, 50(3): 803-812. https://doi.org/10.1016/j.csda.2004.10.005

Liu J, Luan X, Tian X, and Sun Y (2011). Morphological edge detection method of multi-structure and multi-scale based on image fusion in wavelet domain. In: Yang D (Ed.), Informatics in control, automation and robotics. Lecture notes in electrical engineering, Vol 133. Springer, Berlin, Germany. https://doi.org/10.1007/978-3-642-25992-0_91

Lu F, Tang C, Liu T, Zhang Z, and Li L (2023). Multi-attention segmentation networks combined with the Sobel operator for medical images. Sensors, 23(5): 2546. https://doi.org/10.3390/s23052546 **PMid:36904754 PMCid:PMC10007317**

Mao R (2017). A swarm intelligence based medical image edge detection method with adaptive gradient. Journal of Medical Imaging and Health Informatics, 7(5): 1087-1092. https://doi.org/10.1166/jmihi.2017.2141

Miller RK and Zeuch N (1989). Machine vision (competitive manufacturing). Springer, Berlin, Germany.

Prewitt JM (1970). Object enhancement and extraction. In: Lipkin BS (Ed.), Picture processing and Psychopictorics: 75-148. Elsevier, Amsterdam, Netherlands.

Qian HY (2019). Medical image edge detection algorithm based on improved Canny operator. Software Guide, 18(2): 45-48.

She Y (2009). Thresholding-based iterative selection procedures for model selection and shrinkage. Electronic Journal of Statistics, 3: 384-415. https://doi.org/10.1214/08-EJS348

Shokhan MH (2014). An efficient approach for improving canny edge detection algorithm. International Journal of Advances in Engineering and Technology, 7(1): 59-65.

Sun R, Lei T, Chen Q, Wang Z, Du X, Zhao W, and Nandi AK (2022). Survey of image edge detection. Frontiers in Signal Processing, 2: 826967. https://doi.org/10.3389/frsip.2022.826967

Tan W, Tiwari P, Pandey HM, Moreira C, and Jaiswal AK (2020). Multimodal medical image fusion algorithm in the era of big data. Neural Computing and Applications. https://doi.org/10.1007/s00521-020-05173-2

Trujillo-Pino A, Krissian K, Alemán-Flores M, and Santana-Cedrés D (2013). Accurate subpixel edge location based on partial area effect. Image and Vision Computing, 31(1): 72-90. https://doi.org/10.1016/j.imavis.2012.10.005

Ünver HM, Kökver Y, Duman E, and Erdem OA (2019). Statistical edge detection and circular Hough transform for optic disk localization. Applied Sciences, 9(2): 350. https://doi.org/10.3390/app9020350

Wang Q and Ma Q (2024). Super-resolution reconstruction algorithm for medical images by fusion of wavelet transform and multi-scale adaptive feature selection. IET Image Processing, 18: 4297–4309. https://doi.org/10.1049/ipr2.13252

Wei J, Mao S, Dai J, Wang Z, Huang W, and Yu Y (2022). A faster and more accurate iterative threshold algorithm for signal reconstruction in compressed sensing. Sensors, 22(11): 4218. https://doi.org/10.3390/s22114218 **PMid:35684839 PMCid:PMC9185297**

You N, Han L, Liu Y, Zhu D, Zuo X, and Song W (2023). Research on wavelet transform modulus maxima and OTSU in edge detection. Applied Sciences, 13(7): 4454. https://doi.org/10.3390/app13074454

Yunhong S, Shilei Y, Xiaojing Z, and Jinhua Y (2022). Edge detection algorithm of MRI medical image based on artificial neural network. Procedia Computer Science, 208: 136-144. https://doi.org/10.1016/j.procs.2022.10.021

Zhou D and Yuan Z (2024). A new class biorthogonal spline wavelet for image edge detection. ArXiv Preprint ArXiv:2406.08285. https://doi.org/10.48550/arXiv.2406.08285